JOURNAL OF Materials CHEMISTRY

Freeze-dried precursor-based synthesis of new vanadium–molybdenum oxynitrides

Abdelouahad El-Himri, María Cairols, Silvia Alconchel,† Fernando Sapiña,* Rafael Ibañez, Daniel Beltrán and Aurelio Beltrán

Institut de Ciència dels Materials de la Universitat de València, Apartado de Correos 2085 E-46071 València, Spain. E-mail: fernando.sapina@uv.es

Received 30th June 1999, Accepted 27th September 1999

Interstitial vanadium molybdenum oxynitrides in the solid solution series $V_{1-z}Mo_z(O_xN_y)$ ($z=0.0$, 0.2, 0.4, 0.5, 0.6, 0.8, 1.0) have been obtained by direct ammonolysis of precursors resulting from freeze-drying of aqueous solutions of the appropriate metal salts. A study of the influence of the preparative variables on the outcomes of this procedure is presented. Compounds in this series are prepared as single phases by nitridation at 1038 K, followed by fast cooling of the samples. As for the VN and Mo_2N individual nitrides, all the $V_{1-z}Mo_z(O_xN_y)$ compounds in this series have the rocksalt crystal structure, in which the metal atoms are in a fcc arrangement, with N and O atoms occupying octahedral interstitial positions. Cell parameters increase regularly with z, as can be expected taking into account the sizes of V and Mo atoms. The materials have been characterized by X-ray powder diffraction, elemental analysis, scanning electron microscopy and thermogravimetry under oxygen flow. $V_{1-z}Mo_z(O_xN_y)$ grains are aggregates of nanometric spherical particles with typical diameters of *ca.* 20 nm. Their stability in oxygen atmosphere is low but increases with the Mo content.

Introduction

Catalysis is one among the emerging application fields that currently are renewing the interest in transition-metal carbides and nitrides.[1–3] Molybdenum oxynitrides constitute examples of promising materials in this field because of their activity and selectivity in processes involving hydrogen transfer reactions, such as dehydrodenitrogenation (HDN) and dehydrodesulfurization (HDS).[4] In particular, the bimetallic $V_2Mo(O_xN_y)$ phase has been referred to as having superb HDN performance, with an activity higher than that of the VN and Mo_2N individual nitrides or the commercial HDN catalyst.[5,6] Until recently, only this compound, $V_2Mo(O_xN_y)$, was known in the V–Mo–O–N system, and it was originally prepared by ammonolysis of the bimetallic V_2MoO_8 oxide.[5,6] In a recent publication, we have shown, however, the existence of a new definite metallic composition in this system, namely $V_3Mo_2(O_xN_y)$.[7] Both this new oxynitride and the already known $V_2Mo(O_xN_y)$ were prepared by nitridation (under relatively mild conditions) of precursor powders resulting from freeze-drying of aqueous solutions containing both metals in the required nominal stoichiometric ratio. Besides avoiding any problem associated with the need for definite single mixed oxides as precursors,[8–10] such a synthesis approach offers the advantage of quasi-atomic level mixing of the metals in the powder precursor, which decreases the diffusion distances and usually results in very small sized particles. Together with this last feature, the fact that we start from aqueous solutions (which, moreover, allows the exploration of wide metal composition ranges in complex systems) makes this approach especially suitable to be considered for the preparation of catalysts and supported catalysts.

As far as both $V_3Mo_2(O_xN_y)$ and $V_2Mo(O_xN_y)$ are isostructural to VN and Mo_2N individual nitrides (NaCl-type structure), it might be thought that these metallic compositions are simply two points in a $V_{1-z}Mo_z(O_xN_y)$ solid solution series whose ideal limits would be VN and Mo_2N. Given that the catalytic activity in the V–Mo–O–N system will depend on the stoichiometric metal ratio, in the present work we approach the preparation of single phased vanadium molybdenum oxynitrides in the solid solution series $V_{1-z}Mo_z(O_xN_y)$ ($0 \leqslant z \leqslant 1$).

Experimental

Synthesis

Materials used as reagents in this work are NH_4VO_3 (Fluka, 99.0%) and $(NH_4)_6Mo_7O_{24}\cdot 4H_2O$ (Panreac, 99.0%). Starting V or Mo containing solutions were prepared by dissolving the salts in distilled water. Then, these solutions were combined to obtain V–Mo source solutions with a total cationic concentration of 0.50 M, and molar nominal compositions $V:Mo = 1-z:z$ ($z=0.00$, 0.20, 0.40, 0.50, 0.60, 0.80, 1.00). The masses of the different reagents were adjusted to give 5 g of final product. Droplets of these solutions were flash frozen by contact with liquid nitrogen and then freeze-dried at a pressure of 1–10 Pa in a Telstar Cryodos freeze-drier. In this way, dried solid precursors were obtained as amorphous (X-ray diffraction) loose powders.

V–Mo oxynitrides were synthesized by ammonolysis of the amorphous precursor solids (Table 1). The gases employed were NH_3 (99.9%) and N_2 (99.9995%). A sample of the selected precursor (*ca.* 0.5 g) was placed into an alumina boat, which was then inserted into a quartz flow-through tube furnace. The back end of the tube furnace was connected to an acetic acid trap and the front end was connected to the gas line or to a vacuum pump. Prior to initiating the thermal treatment, the tube furnace was evacuated *in vacuo* for 20 min, then purged for 10 min with N_2 and another 20 min with NH_3. Several runs under different experimental conditions were also performed in order to determine the appropriate conditions for the preparation of pure samples. The precursor powder was heated at 5 K min^{-1} to a final temperature (T_f) that was held for a period of time (t_{hold}) under flowing ammonia (50 cm^3 min^{-1}). Then, the solid was cooled at different variable rates (r_c) in the

†Permanent address: Departamento de Química, Facultad de Ingeniería Química, Universidad Nacional del Litoral, Santiago del Estero 2829, 3000 Santa Fe, Argentina.

Table 1 Chemical composition and cell parameters of powder vanadium molybdenum oxynitrides $V_{1-z}Mo_z(O_xN_y)$

z	z (EDAX)	Oxygen (wt%)	Nitrogen (wt%)	Proposed stoichiometry	Cell parameter, a/Å
0.0	—	3.4	19.5	$V(O_{0.19}N_{0.93})$	4.13190(14)
0.2	0.20	5.8	15.5	$V_{0.8}Mo_{0.2}(O_{0.37}N_{0.86})$	4.14309(24)
0.4	0.39	7.5	12.9	$V_{0.6}Mo_{0.4}(O_{0.40}N_{0.80})$	4.15270(23)
0.5	0.51	7.1	12.2	$V_{0.5}Mo_{0.5}(O_{0.40}N_{0.80})$	4.16145(25)
0.6	0.60	5.5	11.5	$V_{0.4}Mo_{0.6}(O_{0.32}N_{0.78})$	4.16608(19)
0.8	0.81	4.1	9.5	$V_{0.2}Mo_{0.8}(O_{0.26}N_{0.68})$	4.17139(18)
1.0	—	4.2	8.2	$Mo(O_{0.29}N_{0.64})$	4.18188(19)

same atmosphere. The different cooling rates were obtained by either turning off the oven and leaving the sample inside (slow, *ca.* 2 K min^{-1}) or by quenching at room temperature (fast, *ca.* 50 K min^{-1}). After cooling, the product was purged with N_2 for 30 min. From these experiments, the appropriate conditions for the preparation of pure samples were found to be 1038 K and use of a fast cooling rate. Thus, for the preparation of pure samples, the precursor powder was heated at 5 K min^{-1} under flowing ammonia (50 cm^3 min^{-1}) to a final temperature of 1038 K. The samples were held at the reaction temperature for 1 h and then quenched to room temperature. After cooling, the resulting solid was purged with N_2 for 30 min. For each composition, several preparations were conducted, to give eventually 1 g of product. A further treatment of 1 h at 1038 K led to the final samples. All products were stored in a desiccator over $CaCl_2$.

Characterization

Elemental analysis. Metal ratios in the solids were determined by energy dispersive X-ray analysis (EDAX) on a JEOL JSM 6300 scanning electron microscope equipped with an Oxford detector with quantification performed using virtual standards on associated Link-Isis software. The operating voltage was 20 kV, and the energy range of the analysis was 0–20 keV. The nitrogen content of the oxynitrides was evaluated by standard combustion analysis (Carlo Erba EA 1108); N_2 and CO were separated in a chromatographic column, and measured using a thermal conductivity detector. The oxygen content was indirectly determined by thermogravimetric analysis (Perkin Elmer TGA 7 system). Table 1 summarizes the results of analyses for the oxynitrides.

X-Ray diffraction. X-Ray powder diffraction patterns were obtained from a Siemens D501 automated diffractometer using graphite-monochromated Cu-Kα radiation. In order to reduce preferred orientation, the samples were dusted through a sieve on the holder surface. Routine patterns for phase identification were collected with a scanning step of 0.08° in 2θ over the angular range 2θ 25–70° with a collection time of 5 s per step. The cell parameters of each product were obtained by profile fitting of the pattern using the method of Le Bail *et al.*[11] as implemented in the FULLPROF program,[12] from patterns collected with a scanning step of 0.02° in 2θ, over a wider angular range (2θ 25–85°), and with a longer acquisition time (10 s per step) in order to enhance statistics. The fits were performed using a pseudo-Voigt peak-shape function. In the final runs, usual profile parameters (scale factors, background coefficients, zero-points, half-width, pseudo-Voigt and asymmetry parameters for the peak-shape) were refined. All graphical representations relating to X-ray powder diffraction patterns were performed using the DRXWin program.[13]

Microstructural characterization. The morphology of both the crystalline precursors and the resulting nitrides and oxynitrides was observed using a scanning electron microscope (Hitachi S-4100) operating at an accelerating voltage of 30 kV. The powders were dispersed in ethanol and treated with ultrasound for 10 min. All the samples were covered with a thin film of gold for better image definition.

Results and discussion

As we have recently shown,[7] both $V_2Mo(O_xN_y)$ and $V_3Mo_2(O_xN_y)$ are relatively easy to obtain by nitridation (1038 K, 2 h) of freeze-dried powder precursors having the required nominal stoichiometry. The syntheses were clean, and both products have the same rocksalt type structure as that found for the individual nitrides VN and Mo_2N. The possible existence of an isostructural $V_{1-z}Mo_z(O_xN_y)$ ($0 \leqslant z \leqslant 1$) solid solution was then considered, which could be of interest in the field of catalysis. At this point, the established fact that different molybdenum nitrides can result from ammonolysis processes depending on both the nature of the molybdenum source and procedural variables,[4b,14] led us to investigate the optimal conditions for obtaining cubic γ-Mo_2N (*i.e.*, the upper limit composition in the hypothetical solid solution) when starting from freeze dried precursors.

On the basis of our previous results in ref. 7 (ammonolysis processes were effective after 2 h at 1038 K), we carried out preliminary treatments for longer times (12 h, to eliminate time as a variable parameter) at 973 and 1073 K. In this way, it was possible to evaluate the influence of other key variables in this type of processes, such as the cooling rate.[5] Fig. 1 shows X-ray diffraction patterns of the products resulting from the ammonolysis of precursors corresponding to the limiting metal compositions $z=0$ and 1, when subjected to slow and fast cooling rates. As can be observed, the cubic phase (VN, JCPDS 35-0768) is obtained at both temperatures for the vanadium-only containing sample ($z=0$), regardless of the cooling rate. However, this latter variable seems of importance in the case of the molybdenum-only containing sample ($z=1$). Thus, slow cooling of samples obtained at both temperatures (973 and 1073 K) results in a mixture of the cubic (γ-Mo_2N, JCPDS 25-1366) and hexagonal (δ-MoN JCPDS 25-1367) phases, the relative amount of the cubic phase increasing with temperature. It seems, therefore, that a competition between the cubic and hexagonal phases exists in Mo containing samples.[15] The hexagonal phase is stabilized at low temperatures, whereas the cubic phase should be stabilized entropically at higher temperatures.

The detection of a certain amount of the hexagonal phase even in the XRD pattern of the sample with $z=1$ prepared at 1073 K might be a consequence of the process $Mo_2N + 1/2N_2 \rightarrow 2$ MoN when the cooling rate is sufficiently slow. Indeed, as shown in Fig. 1, quenching of the samples obtained at 1073 K leads to kinetic stabilization of the cubic phase.

Having established the need for quenching in order to stabilize the cubic phase, we explored in more detail the influence of the temperature on the nature of the resulting phases, *i.e.* we attempted to determine the optimal working temperature range to obtain cubic single phases for each composition in the $V_{1-z}Mo_z(O_xN_y)$ series. Fig. 2 shows X-ray diffraction patterns of the products that result from the

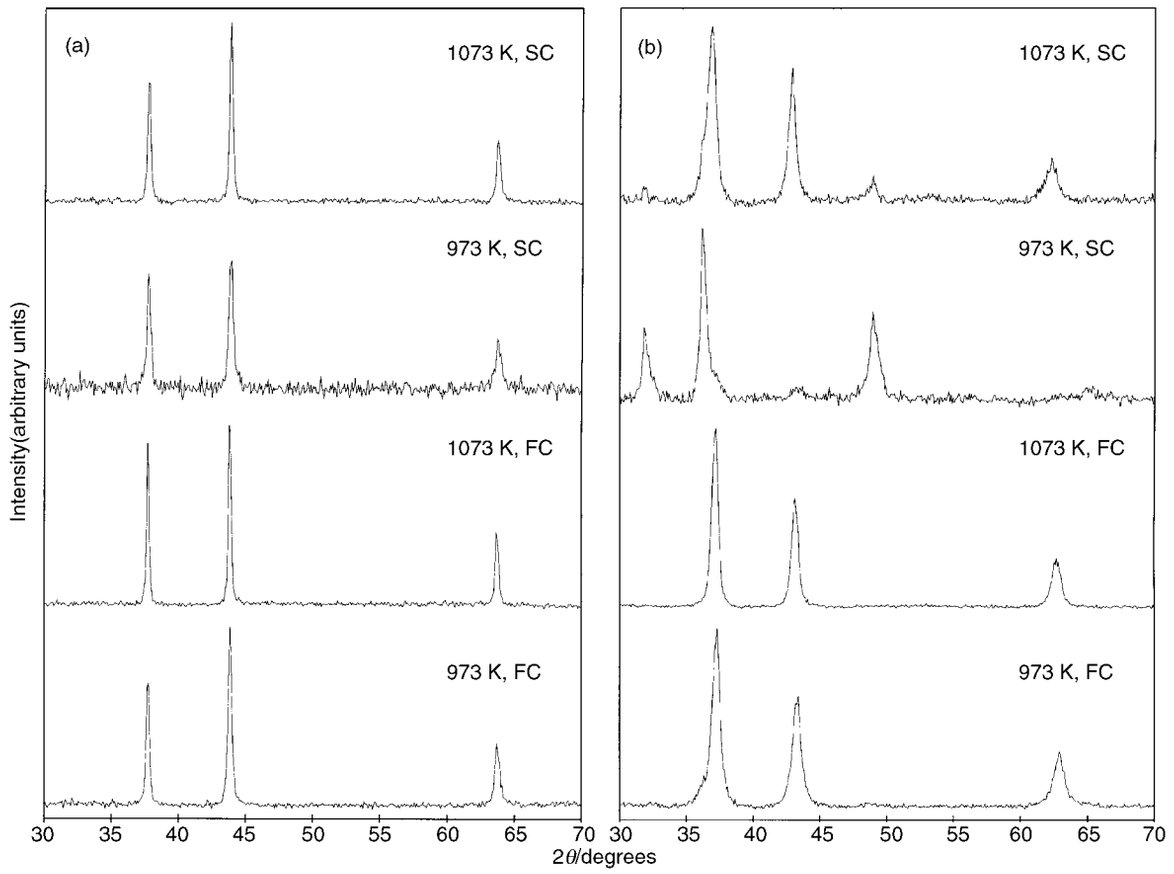

Fig. 1 X-Ray diffraction patterns of the products resulting after ammonolysis of the freeze-dried precursors with $z=0$ (a) and $z=1$ (b) at 973 and 1073 K, for 12 h of thermal treatment and slow or fast cooling rates (SC, FC, respectively).

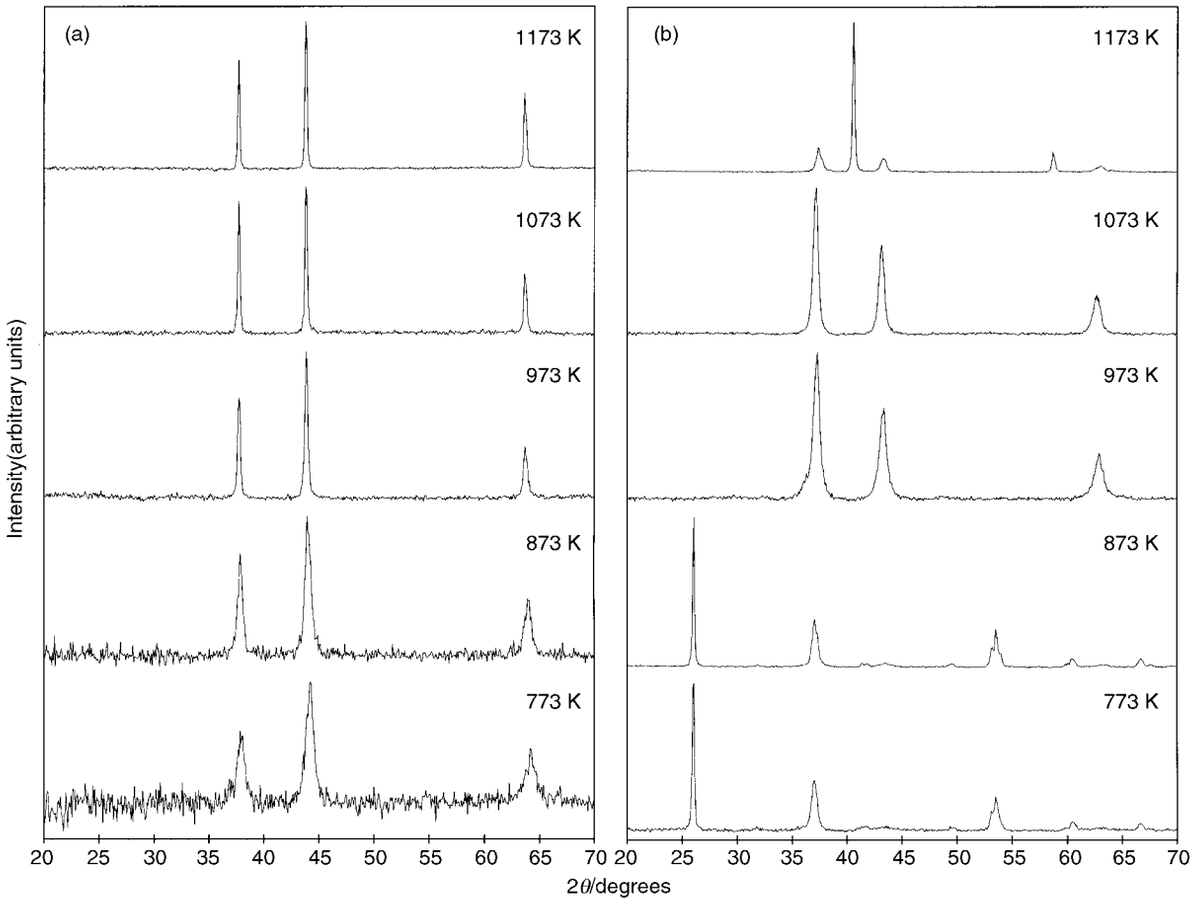

Fig. 2 X-Ray diffraction patterns of the products resulting after ammonolysis of freeze-dried precursors with $z=0$ (a) and $z=1$ (b) at 773, 873, 973, 1073 and 1173 K for 12 h of thermal treatment, and fast cooling rates.

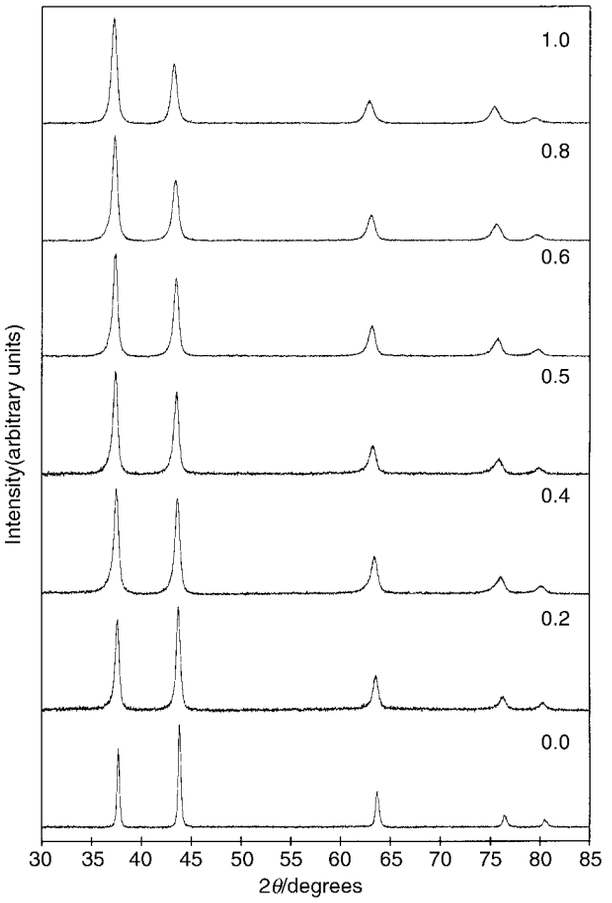

Fig. 3 X-Ray diffraction patterns of the products resulting after ammonolysis of freeze-dried precursors at 1038 K for 2 h, and fast cooling rates. Values of z are indicated.

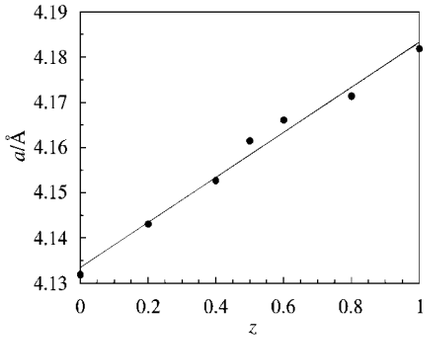

Fig. 4 Cubic cell volume *vs.* composition for $V_{1-z}Mo_z(O_xN_y)$. The solid line corresponds to the best linear fit of the data.

ammonolysis of the precursors corresponding to the limiting metal compositions, $z=0$ and 1, when nitridation was carried out at the temperatures indicated. From these experiments, it can be seen that cubic vanadium oxynitride is obtained as a single phase after nitridation at temperatures as low as 773 K. However, the effective temperature range is limited for the molybdenum oxynitride. Indeed, at temperatures lower than 973 K, ammonolysis does not occur, and only reduction to MoO_2 (JCPDS 32-0671) is observed. On the other hand, metallic molybdenum (JCPDS 04-0809) is the main crystalline product, together with the cubic phase, when the reaction is performed at 1173 K. Indeed, under our synthetic conditions, cubic molybdenum oxynitride only can be obtained as a single phase (*i.e.*, the nitriding character of NH_3 predominates over its reducing character) in a relatively narrow temperature range, from *ca.* 973 to 1073 K.

From the above, we have selected a nitridation temperature of 1038 K and use of fast cooling rates, after 2 h of thermal treatment, as adopted conditions for the preparation of single phases in the $V_{1-z}Mo_z(O_xN_y)$ series. It appears that this temperature is high enough to stabilize the cubic phase for all compositions, while quenching prevents its evolution towards the hexagonal phase. As shown below, the significant shortening of the reaction time, with regard to our preliminary experiments, does not lead to worsening of the results.

Fig. 3 shows XRD patterns corresponding to samples of different compositions in the series $V_{1-z}Mo_z(O_xN_y)$ prepared by nitridation of the freeze-dried precursors under the above conditions. The patterns are characteristic of a rocksalt structure, and cell parameters were calculated by profile fitting of the patterns, using the method of Le Bail *et al.* as implemented in the FULLPROF program[11] (Table 1). Fig. 4 shows the variation of the cell parameter of the cubic structure with the composition. As can be seen, a linear increase in the cell parameter with z is observed, as would be expected taking into account the atomic sizes of V and Mo. The cell dimensions of the synthesized oxynitrides fit well with those previously reported for related phases and for the individual nitrides VN and Mo_2N.

Table 1 shows the results of chemical analysis of the resulting products (black powders). In all cases, the V : Mo ratio is (within experimental error) equal to the nominal value in the corresponding precursor. One aspect that deserves some attention is the proposed nitrogen and oxygen stoichiometry. Prior to this point, we have systematically referred to the VN and Mo_2N limit compositions in the $V_{1-z}Mo_z(O_xN_y)$ solid solution. Both extremes correspond, however, to crystalline phases which are tolerant to a certain non-stoichiometry range, VN_{1-x} ($0 \leqslant x \leqslant 0.15$–$0.20$) and γ-Mo_2N_{1+x} ($-0.2 \leqslant x \leqslant 0.3$).[16] Accordingly, what might be expected for the solid solution is that the N : metal ratio varies from values of *ca.* 0.8–1.0 in the V rich compositions to *ca.* 0.40–0.65 in the Mo rich

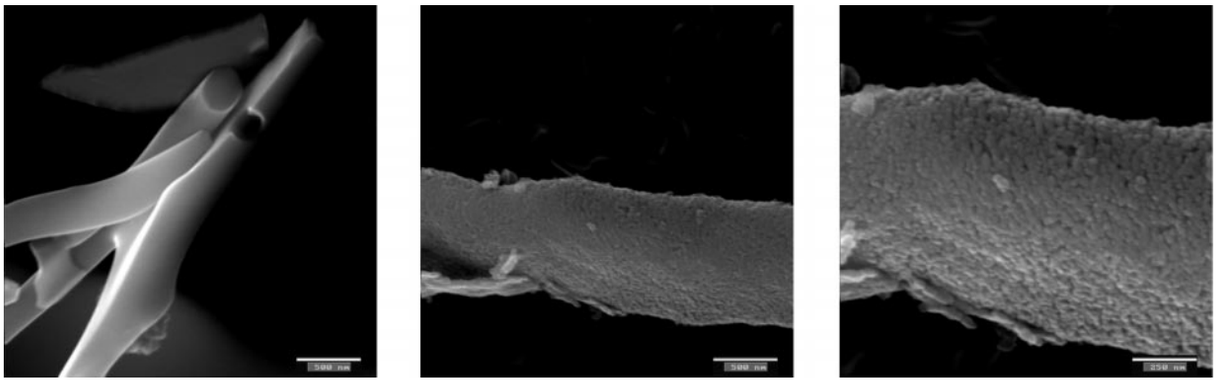

Fig. 5 SEM images showing the microstructure of the amorphous precursor (a) and the oxynitride [(b) and (c)] with $z=0.2$. Scale bars correspond to 500, 500 and 250 nm, respectively.

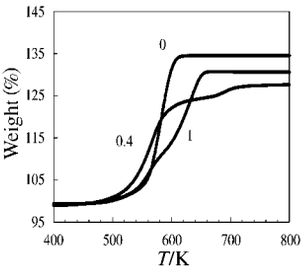

Fig. 6 Characteristic TGA profile corresponding to $V(O_xN_y)$ ($z=0$), $V_3Mo_2(O_xN_y)$ ($z=0.4$) and $Mo(O_xN_y)$ ($z=1$).

compositions. However, such a forecast only makes sense by assuming that the oxygen content in the solids (*i.e.*, the value of x) is variable (*i.e.*, it does not affect the value of y). In fact, previous work on $V_2Mo(O_xN_y)$ and $V_3Mo_2(O_xN_y)$ has shown that the oxygen content depends on the preparation procedures.[5,7] Samples in the $V_{1-z}Mo_z(O_xN_y)$ solid solution tend to be pyrophoric, and so must be passivated (treatment under N_2 atmosphere) prior to their manipulation. The purpose of this passivation is to cover the active surface of the material with a layer of oxide (O_2 present as an impurity in N_2) to prevent oxidation of the bulk. Besides the incorporation of oxygen atoms to interstitial positions, surface oxidation is the main reason for both the oxygen content in the solid (which will depend, therefore, on the procedural variables) and for the constitutional tolerance.

Fig. 5 shows characteristic SEM images corresponding to representative samples. The freeze-dried precursor is comprised of very fine sheets with a typical width of 350 nm [Fig. 5(a)]. The external appearance of the sheets remains practically unchanged during the ammonolysis process yielding $V_{1-z}Mo_z(O_xN_y)$ [Fig. 5(b)], although they now show wrinkled surfaces. SEM images at high magnification [Fig. 5(c)] clearly reveal that $V_{1-z}Mo_z(O_xN_y)$ grains are aggregates of nanometer sized spherical particles with typical diameters around 20 nm.

Fig. 6 shows characteristic TGA profiles for the individual oxynitrides ($z=0$ and 1) and an intermediate composition ($z=0.4$). Except for $z=0$ ($VO_{0.19}N_{0.93}$), oxidation of the bulk samples occurs in a two step process. The oxidation begins in all cases at relatively low temperatures (*ca.* 450–500 K), and is complete between 600 and 750 K, depending on the composition. The final products (800 K) are V_2O_5 (JCPDS 41-1426) for $z=0$, $V_9Mo_6O_{40}$ (JCPDS 34-0527) for $z=0.4$, and MoO_3 (JCPDS 35-0609) for $z=1$. For all the remaining intermediate compositions, a mixture of $V_9Mo_6O_{40}$ and the respective individual oxide (depending on the z value) is obtained. Low temperature oxidation is consistent with the pyrophoric character of these products, this making passivation necessary. Surface oxidation must account to a large extent for the oxygen content of these oxynitrides.

Conclusion

In this work, we have shown the existence of a solid solution series of stoichiometry $V_{1-z}Mo_z(O_xN_y)$ ($0\leqslant z\leqslant 1$) having the rocksalt structure. The $V_2Mo(O_xN_y)$ phase has attracted considerable attention because of its exceptional catalytic activity in processes involving hydrogen transfer reactions. However, such a composition is only one point in the $V_{1-z}Mo_z(O_xN_y)$ series. As far as the catalytic activity in the V–Mo–O–N system must depend on the stoichiometric metal ratio, the synthetic approach reported here could be explored for the optimization of the HDN catalytic properties. Moreover, by starting from aqueous solutions of the metal cations, our approach could open a new way for the preparation of supported HDN oxynitride catalysts.

Acknowledgements

This research was supported by the Spanish Comisión Interministerial de Ciencia y Tecnología (MAT96-1037, PB98-1424). The SCSIE of the Universitat de València is acknowledged for X-ray diffraction, microscopy and analytical facilities. S. A. acknowledges the Fondo para el Mejoramiento de la Calidad Universitaria (FOMEC) and the Universidad del Litoral for a grant for her stay in Spain.

References

1 *The Chemistry of Transition Metal Carbides and Nitrides*, ed. S. T. Oyama, Blackie Academic & Professional, Chapman & Hall, London, 1996, p. 1; *International Symposium on Nitrides*, in *J. Eur. Ceram. Soc.*, ed. Y. Laurent and P. Verdier, 1997, vol. 17, pp. 1773–2037
2 D. H. Gregory, *J. Chem. Soc., Dalton Trans.*, 1999, **3**, 259; R. Niewa and F. J. DiSalvo, *Chem. Mater.*, 1998, **10**, 2733.
3 *High Surface Area Nitrides and Carbides*, in *Catal. Today*, ed. P. W. Lednor, 1992, vol. 15.
4 (*a*) J. C. Schlatter, S. T. Oyama, J. E. Metcalfe and J. M. Lambert, *Ind. Eng. Chem. Res.*, 1988, **27**, 1648; (*b*) C. H. Jaggers, J. N. Michaels and A. M. Stacy, *Chem. Mater.*, 1990, **2**, 150; (*c*) C. W. Colling, J. G. Choi and L. T. Thompson, *J. Catal.* 1996, **160,** 35 and references therein.
5 C. C. Yu, S. Ramanathan, F. Sherif and S. T. Oyama, *J. Phys. Chem.*, 1994, **98**, 13038; C. C. Yu and S. T. Oyama, *J. Solid State Chem.*, 1995, **116**, 205; *J. Mater. Sci.*, 1995, **30**, 4037; R. Kapoor, S. T. Oyama, B. Frühberger and J. G. Chen, *J. Phys. Chem. B*, 1997, **101**, 1543; C. C. Yu, S. Ramanathan and S. T. Oyama, *J. Catal.*, 1998, **173**, 1; S. Ramanathan, C. C. Yu and S. T. Oyama, *J. Catal.*, 1998, **173**, 10.
6 S. T. Oyama, C. C. Yu and F. G. Sherif, *US Pat.*, 5 444 173, 1995.
7 S. Alconchel, F. Sapiña, D. Beltrán and A. Beltrán, *J. Mater. Chem.*, 1999, **9**, 749.
8 H. C. zur Loye, J. D. Houmes and D. S. Bem, in *The Chemistry of Transition Metal Carbides and Nitrides*, ed. S. T. Oyama, Blackie Academic & Professional, Chapman & Hall, London, 1996, p. 154.
9 S. H. Elder, L. H. Doerrer, F. J. DiSalvo, J. B. Parise, D. Gouyomard and J. M. Tarascon, *Chem. Mater.*, 1992, **4**, 928; D. S. Bem and H. C. zur Loye, *J. Solid State Chem.*, 1993, **104**, 467; J. D. Houmes, D. S. Bem and H.-C. zur Loye, *MRS Symposium Proceedings: Covalent Ceramics II: Non-Oxides*, ed. A. R. Barron, G. S. Fischman, M. A. Fury and A. F. Hepp, Materials Research Society, Boston, MA, 1993, vol. 327, p. 153; D. S. Bem, C. P. Gibson and H.-C. zur Loye, *Chem. Mater.*, 1993, **5**, 397; D. S. Bem, H. P. Olsen and H.-C. zur Loye, *Chem. Mater.*, 1995, **7**, 1824; P. Subramanya Herle, N. Y. Vasanthacharya, M. S. Hedge and J. Gopalakrishnan, *J. Alloys Compd.*, 1995, **217**, 22; D. S. Bem, C. M. Lampe-Onnerud, H. P. Olsen and H.-C. zur Loye, *Inorg. Chem.*, 1996, **35**, 581; R. N. Panda and N. S. Gajbhiye, *J. Alloys Compd.*, 1997, **256**, 102.
10 S. Alconchel, F. Sapiña, D. Beltrán and A. Beltrán, *J. Mater. Chem.*, 1998, **8**, 1901.
11 A. Le Bail, H. Duroy and J. L. Fourquet, *Mater. Res. Bull.*, 1988, **23**, 447.
12 J. Rodriguez-Carvajal, FULLPROF Program, personal communication.
13 V. Primo, DRXWin & CreaFit version 2.0: graphical and analytical tools for powder XRD patterns, *Powder Diffract.*, 1999, **14**, 70.
14 R. Marchand, F. Tessier and F. J. DiSalvo, *J. Mater. Chem.*, 1999, **9**, 297.
15 Although the results reported here are referred to the $z=1$ composition, a similar tendency has been observed for the other molybdenum rich samples.
16 P. Ettmayer and W. Lengauer, in *Encyclopedia of Inorganic Chemistry*, ed. R. Bruce King, John Wiley and Sons, Chichester, 1994, p. 2498.

Paper 9/05254B